# Unveiling Chiral Phase Evolution in Rabi Oscillations from a Photonic Setting

Ping Zhang,[1] Qianqian Kang,[1] Yumiao Pei,[1] Zhaoyuan Wang,[1] Yi Hu,[1,*] Zhigang Chen,[1,2,†] and Jingjun Xu[1,‡]
[1]The MOE Key Laboratory of Weak-Light Nonlinear Photonics, TEDA Applied Physics Institute and School of Physics, Nankai University, Tianjin 300457, China
[2]Department of Physics and Astronomy, San Francisco State University, San Francisco, California 94132, USA

(Received 4 February 2020; accepted 5 August 2020; published 15 September 2020)

Rabi oscillation, originally proposed in nuclear magnetic resonance, is a well-known phenomenon associated with a driven two-level system. Although magnetic fields typically can bring about chirality into unusual phenomena such as chiral edge states in the quantum Hall effect, it is not clear if chirality exists in Rabi oscillations. Here we unveil the intrinsic chirality carried by the phase in a Rabi problem. For opposite detuning of the driving field, the phase evolution of the probability amplitude exhibits a mirror symmetry. Consequently, constructive or destructive interference of two off-resonant Rabi processes under different initial conditions is level dependent and symmetry protected. Experimentally, we demonstrate such features in a photonic setting with adjustable detuning, yet our results may prove pertinent to the study of similar phenomena in other driven two-level systems beyond photonics.

DOI: 10.1103/PhysRevLett.125.123201

In his seminal paper, Rabi described a cyclic state transition of a nuclear moment under an external oscillating magnetic field [1]. This milestone finding is the core of technologies including nuclear magnetic resonance spectroscopy and magnetic resonance imaging. In essence, Rabi oscillation is related to a two-level quantum system that interacts with an external periodic driving field. Such a simple system is widely applied to many problems in physics, in the areas such as quantum computing, condensed matter, atomic and molecular physics, nuclear and particle physics, and quantum optics.

In the original Rabi oscillation, both the energy level splitting and the state oscillation are induced by magnetic fields. Magnetic fields (or equivalent synthetic fields) in general can bring about chiral effects as exemplified by the quantum Hall edge states and related topological phenomena [2–5]. In the same vein, chirality should exist as the Rabi oscillation happens. However, to our knowledge, it has never emerged in the probability oscillatory dynamics routinely observed in the control of various quantum or classic states of electrons, photons, phonons, excitons, polaritons, atoms, and molecules [6–18]. The long-term absence of Rabi chirality suggests a possibility that it might be hidden in other dimensions.

In this Letter, we uncover theoretically and demonstrate experimentally the chiral phase evolution in Rabi oscillations. This chiral effect leads to a level-dependent constructive or destructive interference of two off-resonant Rabi processes under different initial conditions. In experiment, such coherent relationship is observed by employing a photonic platform.

The Hamiltonian of a Rabi problem is generally written as $H = -\mathbf{u}\cdot\mathbf{B}$. It describes a spin-1/2 system with a normalized magnetic moment $\mathbf{u} = (\sigma_x, \sigma_y, \sigma_z)$ placed in a classical magnetic field $\mathbf{B}$. The magnetic field consists of a static component along the $x$ direction and a radio-frequency ($v$) component oscillating along the $z$ direction, i.e., $\mathbf{B} = (\omega\hbar/2, 0, -2\varepsilon\cos vt)$ ($\hbar = 1$ hereafter), where $\omega$ and $\varepsilon$ are both constants determining the field strength. The former brings about two nondegenerate states, namely, the spin-up and spin-down states. Their energy difference is $\omega$, also called transition frequency. The oscillating magnetic field induces the transition between the two states. In a rotating frame with an angular speed of $v$ around the $z$ axis, the magnetic field is reshaped as $\mathbf{B}' = (\varepsilon, 0, \Delta/2)$ under the rotating-wave approximation in the energy representation, where $\Delta = \omega - v$ is the detuning of the radio frequency relative to the transition frequency and its value is adopted as positive without loss of generality. The spin-up and -down states in this representation are $|\uparrow\rangle = \binom{1}{0}$ and $|\downarrow\rangle = \binom{0}{1}$, respectively. A Rabi problem can be visualized as a precession of a Bloch vector about the magnetic field $\mathbf{B}'$. For a given state evolving as $c_\uparrow|\uparrow\rangle + c_\downarrow|\downarrow\rangle$, or simply denoted as $\binom{c_\uparrow}{c_\downarrow}$, the polar and azimuthal angles ($\theta$ and $\phi$) of the Bloch vector are obtained by solving $\cos(\theta/2) = |c_\uparrow|$ and $\sin(\theta/2)e^{i\phi} = c_\downarrow|c_\uparrow|/c_\uparrow$ (where $c_\uparrow$ and $c_\downarrow$ are normalized time-dependent complex amplitudes at the upper and bottom levels, respectively, under the condition of $|c_\uparrow|^2 + |c_\downarrow|^2 = 1$). Providing that the sign of the detuning is reversed, a mirrored version of the original Bloch vector motion can be readily found, and its state evolution can be either $\begin{pmatrix} c_\uparrow^* \\ -c_\downarrow^* \end{pmatrix}$ or $\begin{pmatrix} -c_\uparrow^* \\ c_\downarrow^* \end{pmatrix}$. However, the chirality cannot be revealed via the probabilities because they are the same for the two mirrored cases. We thus wonder whether such chirality could be revealed in other dimensions such

 

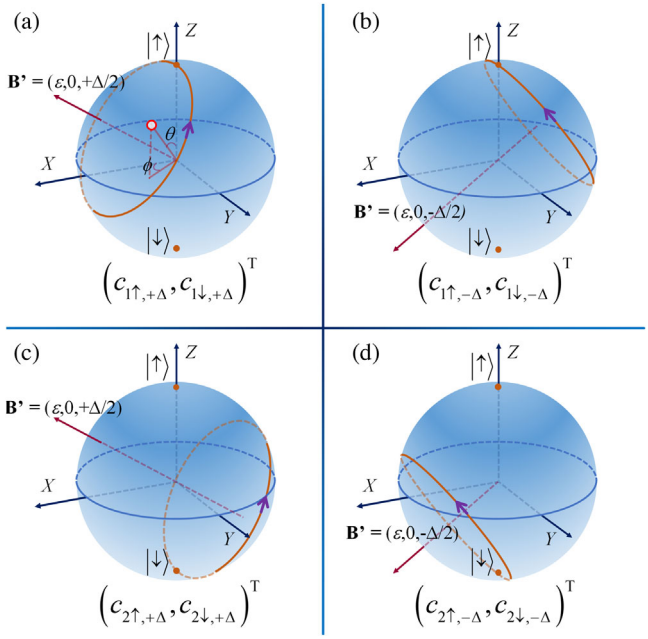


FIG. 1. Bloch sphere illustration of Rabi oscillations under opposite detunings. Procession motion of a Bloch vector starting from the (a),(b) North and (c),(d) South Poles (denoted as red dots), corresponding to the evolution starting from the $|\uparrow\rangle$ and $|\downarrow\rangle$ states, respectively. The associated state vectors are listed below each sphere for positive (left) and negative (right) detunings.

as phase. To this end, a coherent overlapping of two dynamical processes of Rabi oscillation under different initial conditions is considered: the 1st process, represented as $\begin{pmatrix} c_{1\uparrow,\pm\Delta} \\ c_{1\downarrow,\pm\Delta} \end{pmatrix}$ for opposite detunings, starts from the $|\uparrow\rangle$ state; while the 2nd one, represented as $\begin{pmatrix} c_{2\uparrow,\pm\Delta} \\ c_{2\downarrow,\pm\Delta} \end{pmatrix}$, is initiated from the $|\downarrow\rangle$ state. On the Bloch sphere presentation, they undergo circular motion starting from either the North or the South Pole about the corresponding magnetic field (Fig. 1). By considering the symmetry property of the system, their amplitudes at each level have the following relationships: $c^*_{1\uparrow,+\Delta} = c_{1\uparrow,-\Delta}$, $-c^*_{1\downarrow,+\Delta} = c_{1\downarrow,-\Delta}$, $-c^*_{2\uparrow,+\Delta} = c_{2\uparrow,-\Delta}$ and $c^*_{2\downarrow,+\Delta} = c_{2\downarrow,-\Delta}$. Then we can obtain

$$\begin{aligned} \varphi_{\uparrow,+\Delta} + \varphi_{\uparrow,-\Delta} &= 2m\pi + \pi, \\ \varphi_{\downarrow,+\Delta} + \varphi_{\downarrow,-\Delta} &= 2m\pi + \pi, \end{aligned} \tag{1}$$

where $m$ is an integer, $\varphi_{\uparrow,\pm\Delta}$ and $\varphi_{\downarrow,\pm\Delta}$ are the phase delays of the 2nd Rabi process relative to the 1st one at the levels $|\uparrow\rangle$ and $|\downarrow\rangle$, respectively. As shown in Eq. (1), the phase difference in the same energy level is mirror-symmetric about $m\pi + \pi/2$ for opposite detunings. The state evolutions associated with the motions in Fig. 1 are represented by [19]

$$\begin{aligned} c_{1\uparrow,\pm\Delta} &= c^*_{2\downarrow,\pm\Delta} = \cos\Omega t \mp \frac{i\Delta}{2\Omega}\sin\Omega t, \\ c_{1\downarrow,\pm\Delta} &= c_{2\uparrow,\pm\Delta} = -\frac{i\varepsilon}{\Omega}\sin\Omega t, \end{aligned} \tag{2}$$

where $\Omega = \sqrt{\Delta^2/4 + \varepsilon^2}$ is the oscillation frequency. Hence, $\begin{pmatrix} c_{1\uparrow,\pm\Delta} \\ c_{2\uparrow,\pm\Delta} \end{pmatrix}$ and $\begin{pmatrix} c_{1\downarrow,\pm\Delta} \\ c_{2\downarrow,\pm\Delta} \end{pmatrix}$ can form Bloch vectors whose motions are the same with that for the Rabi oscillations initiated from the North and the South Poles, i.e., $\begin{pmatrix} c_{1\uparrow,\pm\Delta} \\ c_{1\downarrow,\pm\Delta} \end{pmatrix}$ and $\begin{pmatrix} c_{2\uparrow,\pm\Delta} \\ c_{2\downarrow,\pm\Delta} \end{pmatrix}$, respectively. Then $\varphi_{\uparrow,\pm\Delta}$ and $\varphi_{\downarrow,\pm\Delta}$ are duplicated to the azimuthal angles of these newly formed Bloch motions [Figs. 2(a) and 2(b)]. Clearly, $\varphi_{\uparrow,+\Delta}$ or $\varphi_{\downarrow,-\Delta}$ is merely valid in the quadrants I and IV, while $\varphi_{\uparrow,-\Delta}$ or $\varphi_{\downarrow,+\Delta}$ in the quadrants II and III. Thus, in the case of positive detuning, the two Rabi processes have constructive and destructive relationships at the levels $|\uparrow\rangle$ and $|\downarrow\rangle$, respectively. Such a level-dependent coherent picture is a direct outcome of the chirality: it is symmetry protected as it can be reversed only via altering the sign of the detuning. Specifically, typical evolutions of the phase difference corresponding to the Bloch vector motion of the single round are presented in Figs. 2(c) and 2(d), while for the case of zero detuning, the phase difference between the two Rabi processes in the same energy level is always $2m\pi \pm \pi/2$, indicating a null contribution from the cross term in the coherent overlapping.

In order to demonstrate the aforementioned level-dependent constructive and destructive relationships, we study the Rabi oscillation in a photonic lattice [20]. The propagation of light in space is analogous to the evolution in time. In the absence of longitudinal modulations, the

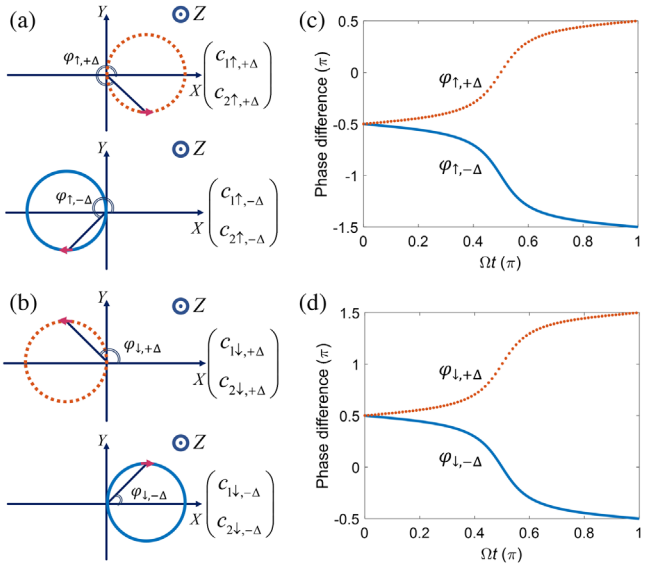


FIG. 2. Coherent relationship between two processes of Rabi oscillations initiated from different energy levels. (a),(b) duplication of the phase difference between the two Rabi processes at either the level $|\uparrow\rangle$ or $|\downarrow\rangle$ in the azimuthal angle of a Bloch vector; (c),(d) evolution of the phase difference calculated by using Eq. (2) with $\varepsilon = 2$ and $\Delta = 0.5$ as a typical example. Blue solid and red dashed lines correspond to the cases of negative and positive detunings, respectively.

photonic lattice is a uniformly distributed waveguide array, in which the wave dynamics can be described by the following coupled-mode equation under the tight-binding condition [21]:

$$id\psi_n/dz = -\mathcal{K}(\psi_{n-1} + \psi_{n+1}), \tag{3}$$

where $\psi_n$ is the probability amplitude in the $n$th waveguide, $z$ is the propagation direction along the waveguide, and $\mathcal{K}$ is the coupling coefficient between two nearest sites. The eigenvalue problem in this system can be solved by assigning $\psi_n = \exp[i(\beta z - qn)]$, where $\beta$ is the propagation constant and $q$ is the quasimomentum. We aim to realize a transition between the state at $q = 0$ and the degenerated state at $q = \pm\pi$ located at the two edges of the Bloch band expressed as $\beta = 2\mathcal{K}\cos q$. For this purpose, a proper longitudinal modulation is required. It can be introduced by recording the nonlinear beating of the two modes via refractive index changes [22]. With such light-induced structures, the Hamiltonian of our system becomes $H = \begin{pmatrix} f(z) & -\mathcal{K} \\ -\mathcal{K} & f(z+\tau/2) \end{pmatrix}$, where $f(z) \propto \cos(2\pi z/\tau)$ indicates the effective written index changes. This Hamiltonian is in accordance with the semiclassical Rabi model as used in our theoretical part. In the absence of the written structure, it describes a two-level system in the tunneling representation, where the spin-up and spin-down states are $|\uparrow\rangle = \frac{1}{\sqrt{2}}\begin{pmatrix} 1 \\ -1 \end{pmatrix}$ and $|\downarrow\rangle = \frac{1}{\sqrt{2}}\begin{pmatrix} 1 \\ 1 \end{pmatrix}$, corresponding to the lattice modes at $q = \pm\pi$ and $q = 0$, respectively.

Following the above analysis, we employ in our experiment a waveguide array fabricated by the titanium in-diffusion technique on the surface of a lithium niobate ($LiNbO_3$) crystal [26] (see the experimental setup in the Supplemental Material [22]). The sample length is 14 mm, and the array period is 6.8 $\mu$m. A broad Gaussian beam (quasi-one-dimensional plane wave) and a cosine-Gaussian beam (sinusoidally modulated) are employed to approximately excite the lattice modes at $q = 0$ and $q = \pm\pi$, respectively. To this end, a phase pattern shown in Fig. 3(a) is imposed on a programmable spatial light modulator (SLM). It picks out three vertical stripe beams from a broad beam ($\lambda = 532$ nm) illuminating the SLM with the assistance of a $4f$ system (consisting of a couple of conjugated cylindrical lenses). Through an objective, the center stripe becomes a Gaussian beam, while the outer two stripes are shaped into a cosine-Gaussian beam at the input of the photonic lattice [Fig. 3(a)]. Both beams are elongated horizontally, covering a large number of waveguides (~60) to only excite the modes around $q = 0$ and $q = \pm\pi$. The longitudinal intensity patterns resulted from their nonlinear beating can be transferred into index changes through the photovoltaic-photorefractive effect [12]. The detuning sign of our Rabi system can be changed at ease by simply changing the initial condition of the writing process. Assuming $r$ is the ratio between the power of the cosine-Gaussian and Gaussian beams, $\Delta > 0$, $\Delta = 0$ and $\Delta < 0$ correspond to $r > 1$, $r = 1$ and $r < 1$, respectively (see the Supplemental Material [22]).

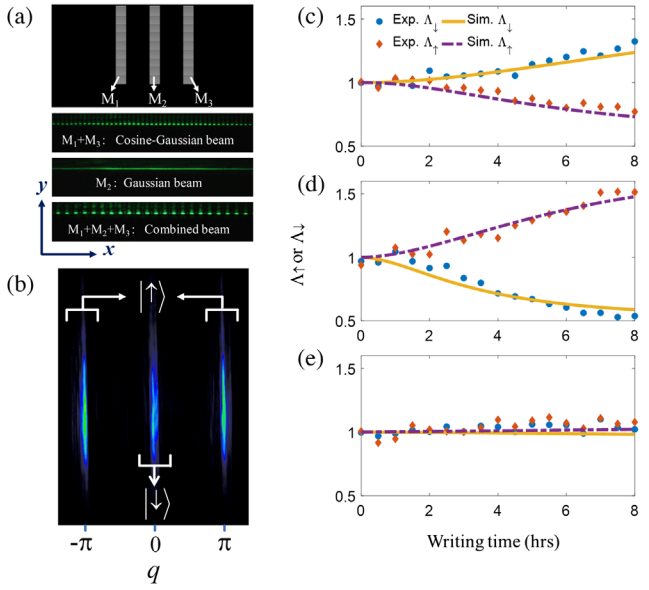


FIG. 3. Experimental demonstration of chirality in photonic Rabi oscillations. (a) Phase patterns (upper panel) imposed on the SLM for alternatively switching on a cosine-Gaussian beam, a Gaussian beam, or their combination (bottom three panels) via displaying different stripes denoted as $M_1$, $M_2$, and $M_3$. (b) Typical spatial spectral distribution at the output associated with the probe beams, where the center (outer) part corresponds to the $|\downarrow\rangle$ ($|\uparrow\rangle$) state. (c)–(e) Coherent relationship (characterized by $\Lambda_j$ that is dimensionless) of two Rabi processes initiated from different levels for the cases of (c) negative, (d) positive, and (e) zero detunings, which are realized by setting the input power ratio between the Gaussian and cosine-Gaussian writing beams as (c) 2:1, (d) 1:2, and (e) 1:1, respectively. Note that the strength of the driving term becomes larger for longer writing time.

To probe such a structure, the same Gaussian beam, cosine-Gaussian beam or their combination is selectively launched, as it can be switched on and off at ease by using the center, outer, or all the stripes of the phase pattern, respectively [Fig. 3(a)]. These optical beams illuminate the Rabi lattice in less than two seconds for each measurement, and are otherwise blocked when only dark illumination for the crystal is needed. As a result of the slow nonlinear response of our sample, the probe beam experiences a linear propagation during probing measurements. The state transition is characterized by transforming the output into the momentum space, where the two lattice modes are well distinguished, residing at the locations with different spatial frequencies, as typically shown in Fig. 3(b). Three output spatial spectra are captured by selectively launching the three input beams. The spectrum associated with the cosine-Gaussian (Gaussian) beam corresponds to the 1st (2nd) Rabi process starting from the level $|\uparrow\rangle$ ($|\downarrow\rangle$), and the third one represents the coherent superposition of the previous two processes. Thus, the powers contained in

the center stripe of the three spectra are $P_1|c_{1\downarrow}|^2$, $P_2|c_{2\downarrow}|^2$ and $|\sqrt{P_1}c_{1\downarrow}+\sqrt{P_2}c_{2\downarrow}|^2$, while those in the outer two stripes are $P_1|c_{1\uparrow}|^2$, $P_2|c_{2\uparrow}|^2$ and $|\sqrt{P_1}c_{1\uparrow}+\sqrt{P_2}c_{2\uparrow}|^2$, where $P_1$ ($P_2$) is the power of the cosine-Gaussian (Gaussian) probe beam, and numbers 1 and 2 indicate the 1st and the 2nd processes, respectively. In measurement, the values of $P_1|c_{1j}|^2$, $P_2|c_{2j}|^2$ and $|\sqrt{P_1}c_{1j}+\sqrt{P_2}c_{2j}|^2$ ($j$ is $\uparrow$ or $\downarrow$) can be obtained by analyzing the three spectra (see a more detailed method in the Supplemental Material [22]). Then the coherent relationship at each level is readily obtained by calculating the parameter $\Lambda_j=|\sqrt{P_1}c_{1j}+\sqrt{P_2}c_{2j}|^2/(P_1|c_{1j}|^2+P_2|c_{2j}|^2)$, which indeed shows a comparison between coherent and incoherent superpositions of the two Rabi processes initiated from either level.

In the first experiment, the power ratio of the Gaussian and cosine-Gaussian beams is set as 2:1 and their total power is 2.2 $\mu$W. Thanks to the slow nonlinear response of our crystal, we can obtain various strengths of the driving term by simply altering the length of writing time [27] (see the Supplemental Material [22]). Nevertheless, negatively detuned Rabi lattices are always expected, since the detuning sign is merely determined by the input power ratio. Thus, although the light-induced index change becomes stronger for longer writing time, the probed two Rabi processes always exhibit a constructive (destructive) interference at the level $|\downarrow\rangle$ ($|\uparrow\rangle$) [Fig. 3(c)]. As analyzed before, such a level-dependent coherent picture is symmetry protected and is only reversed by using an opposite detuning.

Next, we switch the power ratio of the Gaussian and cosine-Gaussian beams to 1:2 and keep the total input power and all other excitation conditions unchanged. Clearly, the coherent relationships at both levels are reversed [Fig. 3(d)]. The values of $\Lambda_j$ are not exactly exchanged for the same writing period as compared with that in Fig. 3(c), since the nonlinear response time of the crystal varies with input beam intensity of different profiles. Finally, for the case of zero detuning realized by using the Gaussian and cosine-Gaussian writing beams with an equal power, the two Rabi processes under test exhibit nearly an absolute phase delay of $\pi/2$ [Fig. 3(e)]. Our experimental results are well corroborated by numerical simulations (see the theoretical model in the Supplemental Material [22]).

For particularly high modulation of the driving field, the rotation wave approximation cannot be applied. In the presence of the high frequency terms, the level-dependent coherent relationship becomes invalid for the case of negative detuning [Fig. 4(a)], but still exists for positive detuning [Fig. 4(b)]. Thus, one can employ the latter case to demonstrate the chirality. In the next experiment, the power of the combined beam is turned up to 4.2 $\mu$W for inducing higher index changes, yet the ratio of the Gaussian and cosine-Gaussian beams is still 1:2. The measured results presented in Figs. 4(c)–4(d) clearly show the level-dependent coherent relationship.

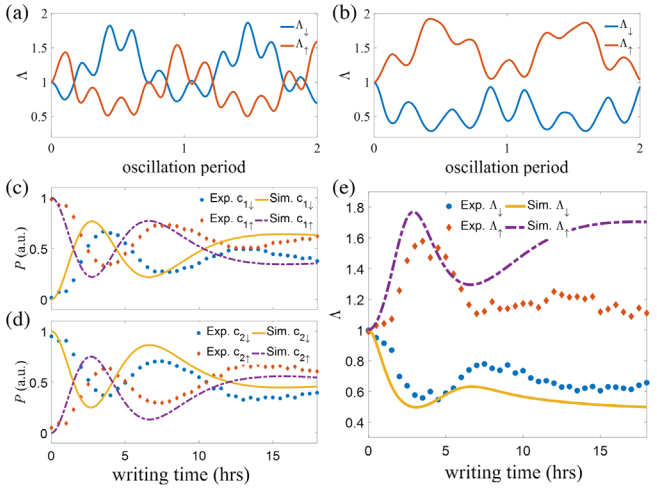


FIG. 4. Coherent relationship of two Rabi oscillations initiated from different levels under a high modulation of the driving term. (a),(b) Simulations along propagation for negative (a) and positive (b) detunings; (c),(d) measured and simulated power ratio in each level at the output for different writing time of the longitudinal index changes probed by the cosine-Gaussian (c) and Gaussian (d) beam; (e) the coherent relationship of the two Rabi processes shown in (c) and (d).

In conclusion, we have revealed the chirality hidden in the phase evolution of Rabi oscillations. Our analysis clearly shows that there is a mirror symmetry of such evolutions for the cases of opposite detunings. This property can be read out by the level-dependent constructive and destructive interferences of two Rabi processes initiated from different levels. The experiments performed in a photonic platform further verify the symmetry-protected coherent effect. Our study may bring about new insights and perspectives to the conventional Rabi problem applicable to fundamental physics and technological implementation involving driven two-level systems.

We acknowledge Detlef Kip, Christian E. Rüter, and Cibo Lou for offering the nonlinear sample. We acknowledge financial support from the National Key R&D Program of China (2017YFA0303800), the National Natural Science Foundation of China (NSFC) (61575098, 91750204), and the 111 Project in China (B07013).

*yihu@nankai.edu.cn
†zgchen@nankai.edu.cn
‡jjxu@nankai.edu.cn

[1] I. I. Rabi, Phys. Rev. **51**, 652 (1937).
[2] R. B. Laughlin, Phys. Rev. B **23**, 5632 (1981).
[3] B. I. Halperin, Phys. Rev. B **25**, 2185 (1982).
[4] L. Lu, J. D. Joannopoulos, and M. Soljačić, Nat. Photonics **8**, 821 (2014).

[5] N. Goldman, G. Juzeliūnas, P. Öhberg, and I. B. Spielman, Rep. Prog. Phys. **77**, 126401 (2014).
[6] J. R. Petta, A. C. Johnson, J. M. Taylor, E. A. Laird, A. Yacoby, M. D. Lukin, C. M. Marcus, M. P. Hanson, and A. C. Gossard, Science **309**, 2180 (2005).
[7] E. A. Chekhovich, M. N. Makhonin, A. I. Tartakovskii, A. Yacoby, H. Bluhm, K. C. Nowack, and L. M. K. Vandersypen, Nat. Mater. **12**, 494 (2013).
[8] D. D. Awschalom, L. C. Bassett, A. S. Dzurak, E. L. Hu, and J. R. Petta, Science **339**, 1174 (2013).
[9] R. J. Warburton, Nat. Mater. **12**, 483 (2013).
[10] D. D. Awschalom, R. Hanson, J. Wrachtrup, and B. B. Zhou, Nat. Photonics **12**, 516 (2018).
[11] F. A. Zwanenburg, A. S. Dzurak, A. Morello, M. Y. Simmons, L. C. L. Hollenberg, G. Klimeck, S. Rogge, S. N. Coppersmith, and M. A. Eriksson, Rev. Mod. Phys. **85**, 961 (2013).
[12] K. Shandarova, C. E. Rüter, D. Kip, K. G. Makris, D. N. Christodoulides, O. Peleg, and M. Segev, Phys. Rev. Lett. **102**, 123905 (2009).
[13] B. Terhalle, A. S. Desyatnikov, D. N. Neshev, W. Krolikowski, C. Denz, and Y. S. Kivshar, Phys. Rev. Lett. **106**, 083902 (2011).
[14] A. D. O'Connell, M. Hofheinz, M. Ansmann, R. C. Bialczak, M. Lenander, E. Lucero, M. Neeley, D. Sank, H. Wang, M. Weides, J. Wenner, J. M. Martinis, and A. N. Cleland, Nature (London) **464**, 697 (2010).
[15] A. Schülzgen, R. Binder, M. E. Donovan, M. Lindberg, K. Wundke, H. M. Gibbs, G. Khitrova, and N. Peyghambarian, Phys. Rev. Lett. **82**, 2346 (1999).
[16] L. Dominici, D. Colas, S. Donati, J. P. Restrepo Cuartas, M. De Giorgi, D. Ballarini, G. Guirales, J. C. Lopez Carreno, A. Bramati, G. Gigli, E. del Valle, F. P. Laussy, and D. Sanvitto, Phys. Rev. Lett. **113**, 226401 (2014).
[17] M. R. Matthews, B. P. Anderson, P. C. Haljan, D. S. Hall, M. J. Holland, J. E. Williams, C. E. Wieman, and E. A. Cornell, Phys. Rev. Lett. **83**, 3358 (1999).
[18] S. Bertaina, S. Gambarelli, T. Mitra, B. Tsukerblat, A. Müller, and B. Barbara, Nature (London) **453**, 203 (2008).
[19] M. O. Scully and M. S. Zubairy, *Quantum Optics* (Cambridge University Press, Cambridge, England, 1997).
[20] D. N. Christodoulides, F. Lederer, and Y. Silberberg, Nature (London) **424**, 817 (2003).
[21] D. N. Christodoulides and R. I. Joseph, Opt. Lett. **13**, 794 (1988).
[22] See Supplemental Material at http://link.aps.org/supplemental/10.1103/PhysRevLett.125.123201 for the method of generating longitudinal modulation, which includes Refs. [23–25].
[23] A. Smerzi, S. Fantoni, S. Giovanazzi, and S. R. Shenoy, Phys. Rev. Lett. **79**, 4950 (1997).
[24] S. Raghavan, A. Smerzi, S. Fantoni, and S. R. Shenoy, Phys. Rev. A **59**, 620 (1999).
[25] G. Bartal, O. Manela, and M. Segev, Phys. Rev. Lett. **97**, 073906 (2006).
[26] V. Gericke, P. Hertel, E. Krätzig, J. P. Nisius, and R. Sommerfeldt, Appl. Phys. B **44**, 155 (1987).
[27] E. Smirnov, M. Stepic, C. E. Rüter, V. Shandarov, and D. Kip, Opt. Lett. **32**, 512 (2007).